Uniform exciton fluorescence from individual molecular nanotubes immobilized on solid substrates

Eisele, Doerthe M.; Knoester, Jasper; Kirstein, Stefan; Rabe, Juergen P.; Vanden Bout, David A.; Rabe, Jürgen P.

Published in:
Nature Nanotechnology

DOI:
10.1038/nnano.2009.227

Publication date:
2009

LETTERS
PUBLISHED ONLINE: 30 AUGUST 2009 | DOI: 10.1038/NNANO.2009.227
nature nanotechnology

Uniform exciton fluorescence from individual molecular nanotubes immobilized on solid substrates

Dörthe M. Eisele[1], Jasper Knoester[2], Stefan Kirstein[1], Jürgen P. Rabe[1]* and David A. Vanden Bout[3]*

Self-assembled quasi one-dimensional nanostructures of π-conjugated molecules[1–15] may find a use in devices owing to their intriguing optoelectronic properties, which include sharp exciton transitions[1–5], strong circular dichroism[5–7], high exciton mobilities[8,9] and photoconductivity[10]. However, many applications require immobilization of these nanostructures on a solid substrate, which is a challenge to achieve without destroying their delicate supramolecular structure. Here, we use a drop-flow technique to immobilize double-walled tubular J-aggregates of amphiphilic cyanine dyes without affecting their morphological or optical properties. High-resolution images of the topography and exciton fluorescence of individual J-aggregates are obtained simultaneously with polarization-resolved near-field scanning optical microscopy. These images show remarkably uniform supramolecular structure, both along individual nanotubes and between nanotubes in an ensemble, demonstrating their potential for light harvesting and energy transport.

Double-walled tubular J-aggregates of amphiphilic cyanine dyes are a particularly interesting class of self-assembled molecular aggregates[7,16]. Similar to the highly efficient photosynthetic antenna systems of green sulphur bacteria[8,17,18], they contain thousands of molecules, packed in a cylindrical geometry with a diameter on the order of 10 nm and a length that may extend to micrometres[5,7]. The interaction between the optical transitions of the molecules within the aggregates leads to delocalized electronic excitations, Frenkel excitons, which determine their fascinating opto-electronic properties[1,5]. It remains a challenge, however, to immobilize non-destructively such self-assembled supramolecular structures on solid substrates, and to determine their uniformity both within a single aggregate as well as between different aggregates within an ensemble.

Here, we report on tubular J-aggregates of the amphiphilic cyanine dye 3,3′-bis(2-sulphopropyl)-5,5′,6,6′-tetrachloro-1,1′-dioctylbenzimidacarbocyanine (C8S3) (Fig. 1a,b)[5,7,19]. The combination of the stacking of the dyes' π-conjugated units and hydrophobic interactions of the alkyl chains in aqueous solution yields double-walled nanotubes, as observed in cryo-transmission electron microscopy (TEM) images[7]. The details of the molecular packing determine the nature of the delocalized exciton states[1,5]. Here, the packing leads to J-aggregates, which exhibit highly fluorescent exciton transitions, narrowed and redshifted compared with the monomer, where the two peaks in the fluorescence spectrum have been previously attributed to the inner and outer wall of the tubular aggregate[5,19] (Fig. 1c,d). The redshifted J-bands clearly indicate strong excitation transfer interactions between the individual molecules, which is a prerequisite for efficient energy transport.

Because the optical properties of J-aggregates depend sensitively on the supramolecular structure, polarization-resolved fluorescence near-field scanning optical microscopy (NSOM)[20–22] is a powerful tool for the investigation of the uniformity of individual tubular J-aggregates on solid substrates. To immobilize the aggregates from solution, a drop-flow technique (see Methods) was developed that isolates the nanotubular aggregates sparsely across the solid substrate as shown by scanning force microscopy (SFM) (Fig. 2a). The height analysis of the SFM images reveals a distribution with two distinct average thicknesses of (12 ± 2) nm and (24 ± 2) nm (see Methods and Supplementary Information). The smaller value is consistent with cryoTEM data obtained for frozen solutions of the tubular aggregates (13 ± 0.5) nm) (ref. 7). The larger structures are attributed to bundles consisting of two to four tubes[7]. Figure 2b shows that the fluorescence spectrum from an ensemble of tubes in solution is almost identical to that acquired from an ensemble on a solid substrate. This strongly suggests that the supramolecular structure is unchanged upon deposition, because the exciton energies and optical transition strengths depend sensitively on the aggregates' structure[5]. We found that the traditional spin-coating method, the most common technique to deposit molecular aggregates onto solid substrates, does not maintain the supramolecular structure (see Supplementary Information).

NSOM images of both topography and fluorescence of the nanotubes isolated on the substrate were collected simultaneously. The aggregates were excited in the near-field and the fluorescence collected in the far-field. Figure 3a,b presents NSOM images, in which the fluorescence intensities were probed with an optical resolution (see Supplementary Information) of better than 70 nm. The images demonstrate that the tubes' fluorescence is strictly correlated with the topography. The simultaneous recording of both topography and fluorescence together with the high resolution of the NSOM enabled us to spatially probe variations of the structure within and between individual aggregates. This is in contrast to previous studies of individual aggregates with NSOM and confocal microscopy[4,20,23–25], which were often complicated by a broad and sometimes hard to control distribution of aggregate morphologies.

The most obvious distinction in both topography and fluorescence images (Fig. 3c,d) is between the individual aggregates and the bundled ones. The larger heights of the latter in the topography clearly correlate with higher fluorescence intensities; in fact the image (Fig. 3e) shows that the intensity (Fig. 3f) of a bundled aggregate is essentially the sum of the intensities of the two merging individual aggregates $[I_{\text{bundle}}/\Sigma I_{\text{individual}} = (0.98 \pm 0.10)]$, indicating no significant quenching of the fluorescence intensity in the bundled aggregates (see

[1]Department of Physics, Humboldt-Universität zu Berlin, Newtonstraße 15 D-12489 Berlin, Germany, [2]Center for Theoretical Physics and Zernike Institute for Advanced Materials, University of Groningen, Nijenborgh 4, NL-9747 AG Groningen, The Netherlands, [3]Department of Biochemistry and Chemistry and Center for Nano and Molecular Science and Technology, 1 University Station, University of Texas, Austin, Texas 78731, USA. *e-mail: rabe@physik.hu-berlin.de; dvandenbout@cm.utexas.edu

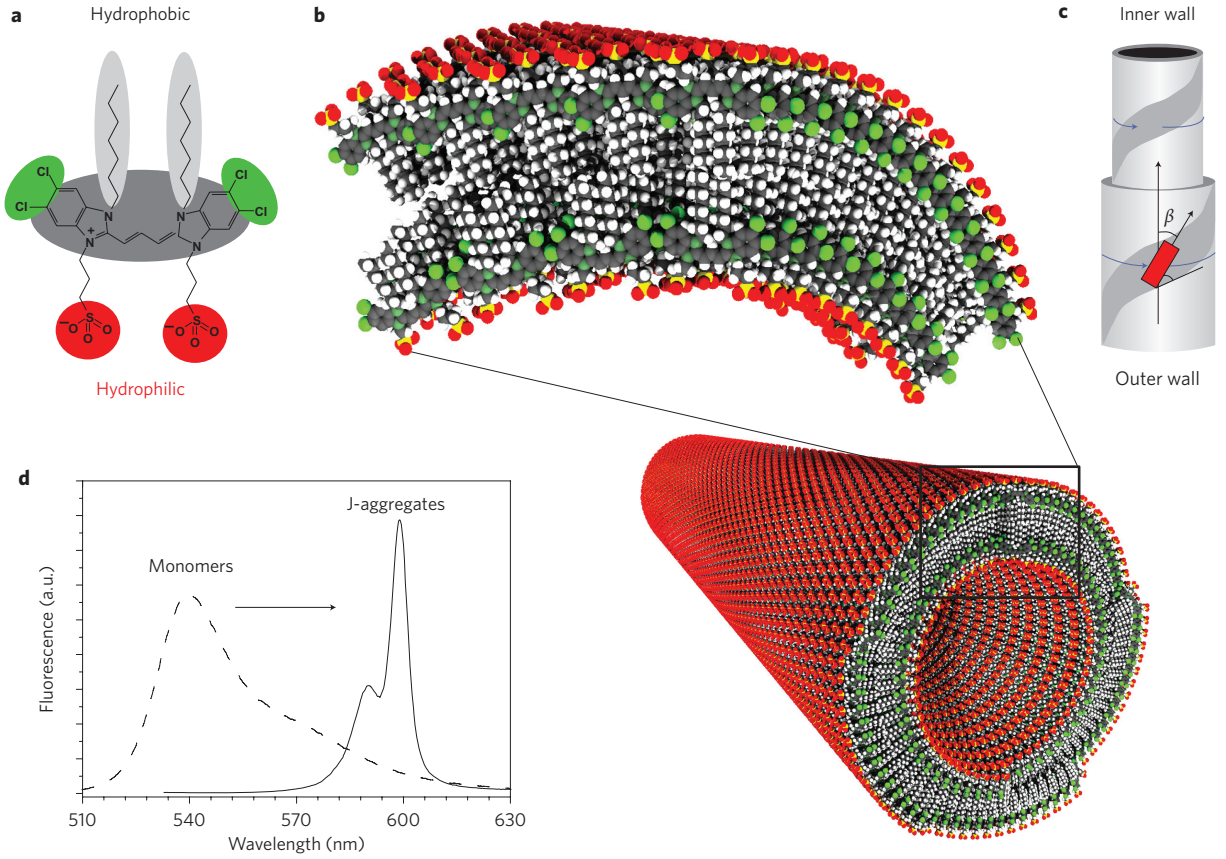

Figure 1 | Cylindrical chiral double-walled nanotubular J-aggregates of an amphiphilic cyanine dye molecule. a, 3,3′-bis(2-sulphopropyl)-5,5′,6,6′-tetrachloro-1,1′-dioctylbenzimidacarbocyanine (C8S3) monomer. **b**, Schematic of the self-assembled nanotube showing the double-walled structure with the alkyl chains at the interior of the bilayer. **c**, Schematic showing the orientation, β, of the transition dipole of the monomer relative to the long axis of the nanotube. The grey band demonstrates how the monomers wrap around the aggregate in both the inner and outer walls. **d**, Fluorescence spectra of the monomer's solution and the aggregate's solution showing the narrowed and redshifted transitions typical for J-aggregates. The two main aggregate fluorescence peaks can be assigned to separate exciton transitions for the inner and outer walls[5,19].

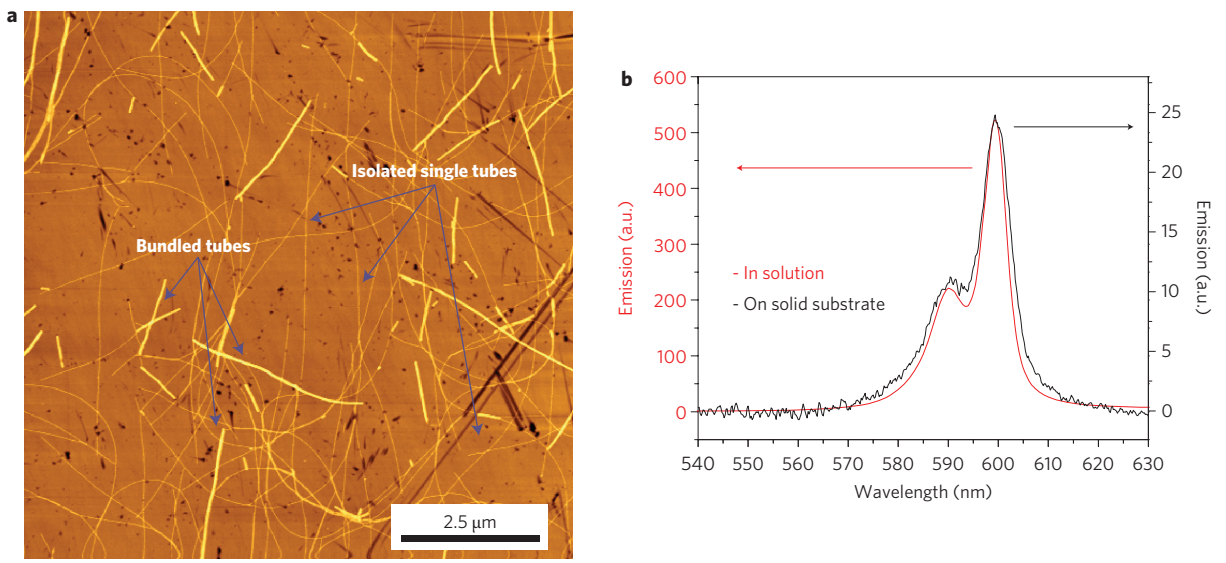

Figure 2 | Immobilization of tubular J-aggregates on a solid substrate. a, Scanning force microscopy image of the tubular aggregates immobilized on a quartz substrate. Long nanostructures with two distinct heights are clearly visible. The thinner objects are attributed to single tubular aggregates and the thicker ones to bundles of such aggregates. **b**, Fluorescence spectra of the aggregates' ensemble in solution (red) and on the solid substrate (black), normalized to the maxima. The agreement between the two spectra indicates that the supramolecular structure of the aggregate remains intact upon deposition onto the solid substrate.

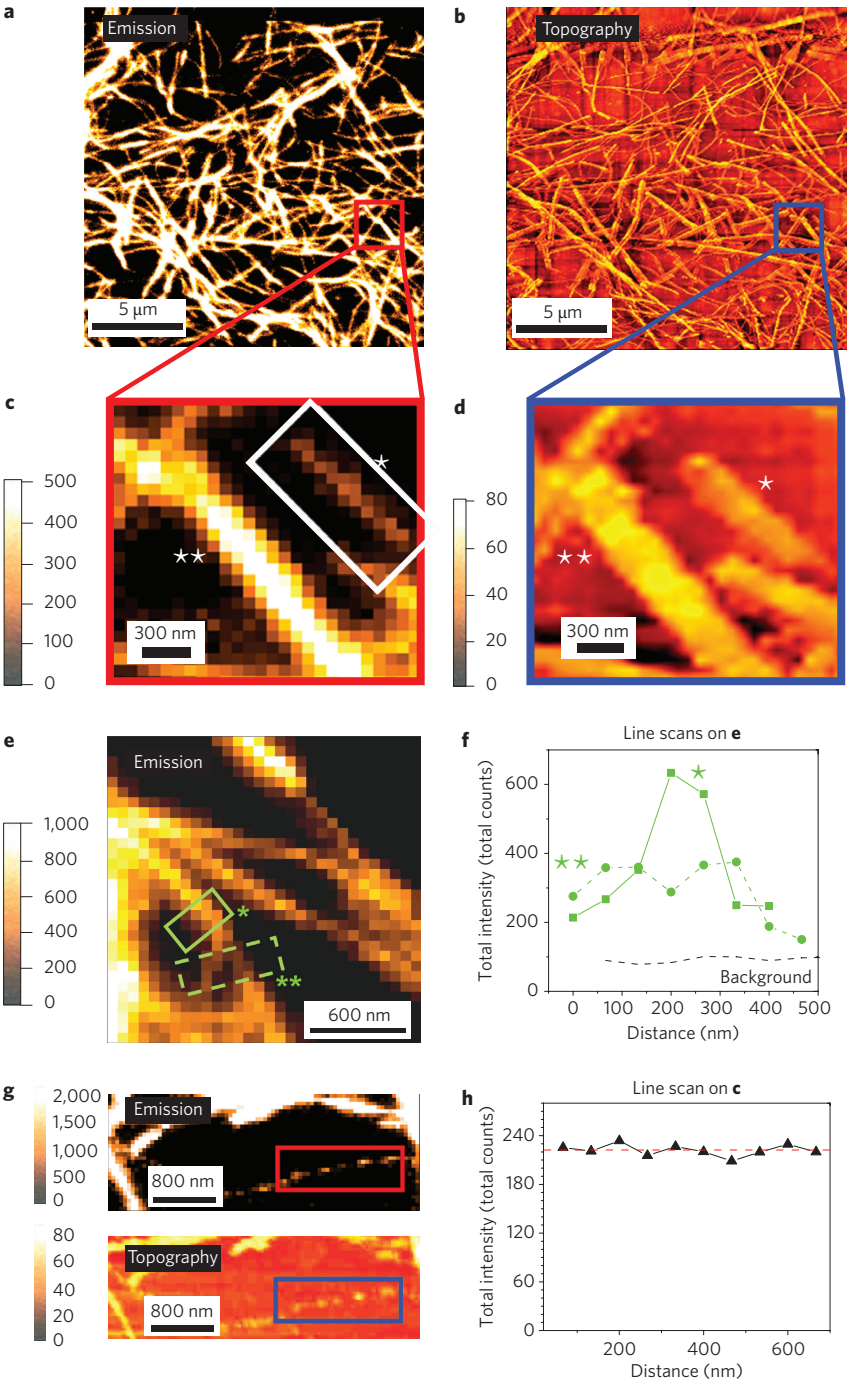

Figure 3 | Fluorescence and topography NSOM images of the tubular aggregates. a,b, Total fluorescence (**a**) and topography (**b**). The fluorescence is clearly correlated with the topography, indicating that the emission is originating from the aggregates. **c,d**, Individual aggregates (*) and bundles (**) are clearly visible in the expanded portions of **c** and **d** of the emission and topography images, respectively. **e**, Fluorescence of individual aggregates that merge into a bundled aggregate. **f**, Line scans perpendicular to the aggregates in **e**, averaging over 200 nm. The ratio of the total intensities of the bundled aggregate (*) and of the sum of the total intensity of the two separated aggregates (**) is 0.98 ± 0.10 indicating no significant quenching of the fluorescence in the bundled aggregates. **g**, Some images reveal aggregates that have been broken upon deposition; the pieces of such broken tubes are visible in both the emission and the topography. **h**, Fluorescence along the individual tube highlighted in image **c**. The red line indicates the average fluorescence along the nanostructure. The small fluctuations in intensity are consistent with the expected photon counting noise.

Supplementary Information). Finally, less than 10% of the individual aggregates displayed large spatial variations in their fluorescence intensities, with regions that appear to have little or no fluorescence (Fig. 3g). The corresponding topographic image reveals that these aggregates are no longer morphologi-cally intact.

Although both individual aggregates and bundled aggregates show interesting optical properties with strongly fluorescent J-bands, we focused further studies on the supramolecular structure of individual, morphologically intact double-walled nanotubular aggregates, as these present the simplest quasi-one-dimensional excitonic model system. The fluorescence intensity along a tube is highly uniform, as demonstrated by a representative line scan along a tube segment (Fig. 3c,h). Generally, the observed intensity fluctuation along the tube segments was found to be consistent with the expected Poisson

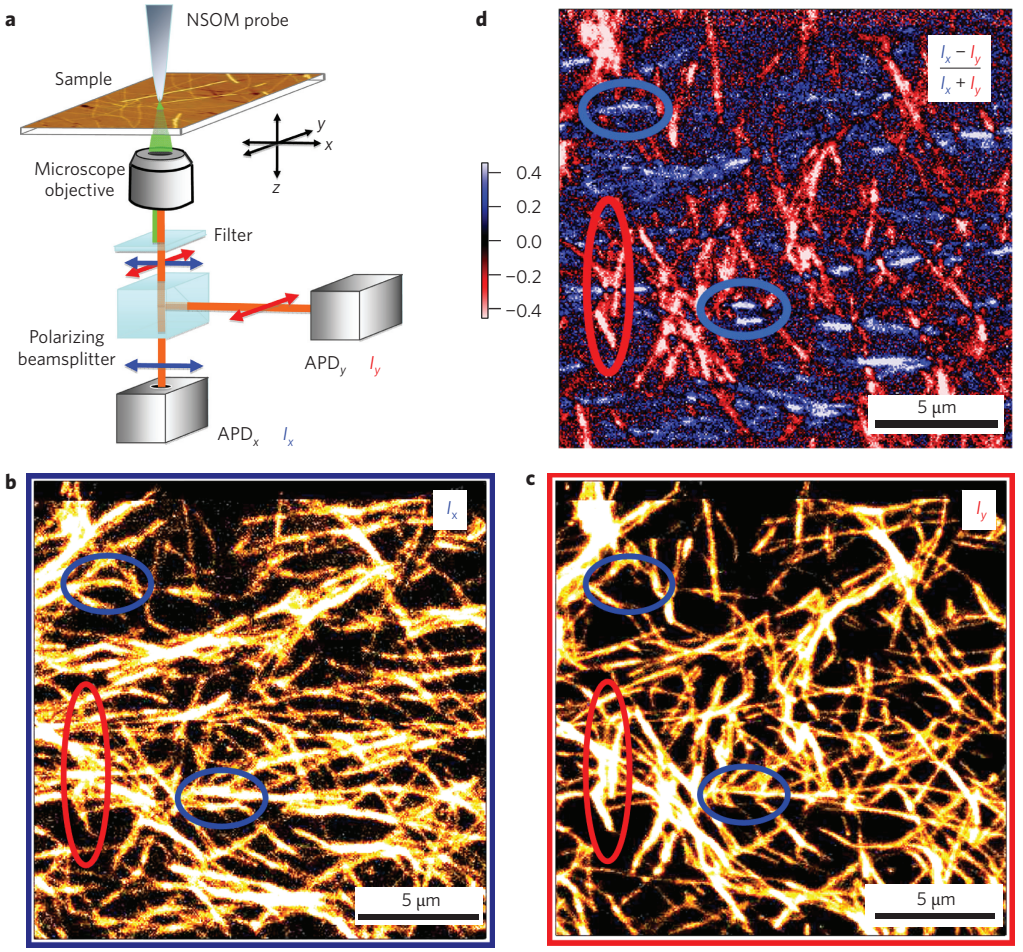

Figure 4 | Polarized fluorescence NSOM images of the tubular aggregates. a, Schematic of the collection geometry in which images of the fluorescence intensity, *I*, in two orthogonal polarizations are collected simultaneously by separate avalanche photodiodes (APD). **b**, NSOM image of the horizontally polarized fluorescence. **c**, NSOM image of the vertically polarized fluorescence. The red (blue) ellipses highlight aggregates for which emission is dominated by the vertical (horizontal) channel; these are all oriented approximately in the vertical (horizontal) direction. **d**, NSOM image of the fluorescence dichroism *D* defined in equation (2). The vertically oriented aggregates show negative dichroism (red) and the horizontal ones are positive (blue).

distribution from photon counting (see Supplementary Information). Its standard deviation of 7% indicates a spatially highly uniform supramolecular structure of the individual aggregates.

The polarization of the fluorescence with respect to the tubular axis provides an even more critical probe of the uniformity of the aggregate's structure, because it is extremely sensitive to the molecular packing, in particular to the angle β between the transition dipoles of individual molecules and the tube's long axis[5] (Fig. 1c). To investigate the polarization properties, the emission was collected in two mutually perpendicular polarization directions (x and y) that correspond to the horizontal and vertical directions in the images (Fig. 4a). Figure 4b,c displays the simultaneously collected fluorescence intensities, I_x and I_y, which clearly demonstrate a strong correlation between the orientation of the tubes on the substrate and the polarization of their fluorescence: the aggregates oriented along the x-axis (y-axis) are brightest in the x-polarized (y-polarized) image.

The polarization of the individual aggregates was quantified using the reduced linear emission dichroism

$$D = \frac{I_x - I_y}{I_x + I_y} \qquad (1)$$

Figure 4d displays an image of D, which allows one to correlate the polarization properties to the orientation of the aggregates on the substrate, characterized by the angle Φ between the axis of the aggregates and the x-axis of the image. If the aggregates all have the same emission dipole moments, their dichroism will depend on the angle Φ. The cylindrical symmetry of a tubular aggregate dictates general selection rules such that it has emission components parallel and perpendicular to its axis[5]. From these selection rules, one finds that for a tubular aggregate oriented at the angle Φ

$$D(\Phi) = a\cos(2\Phi) \qquad (2)$$

where a depends on the relative intensities of the emission components that are polarized parallel and perpendicular with respect to the aggregate's axis. If a were the same for all aggregates, this would be a strong indication that their exciton spectra and thus their supramolecular structures are spatially uniform and identical for all aggregates. This would provide hitherto unknown information on the variation of the emission strengths of the exciton states in individual tubes along the directions parallel and perpendicular to their axes.

Figure 5 displays the dichroism D for 18 tubes plotted against their orientation Φ on the surface. Also shown is a fit to equation (2), which yields $a = 0.67 \pm 0.04$. The quality of the fit clearly demonstrates that indeed there is no significant variation between the different aggregates within the ensemble. The fact that a is smaller than unity indicates that a portion of the emission is polarized perpendicular to the tube's axis. This agrees with model calculations performed

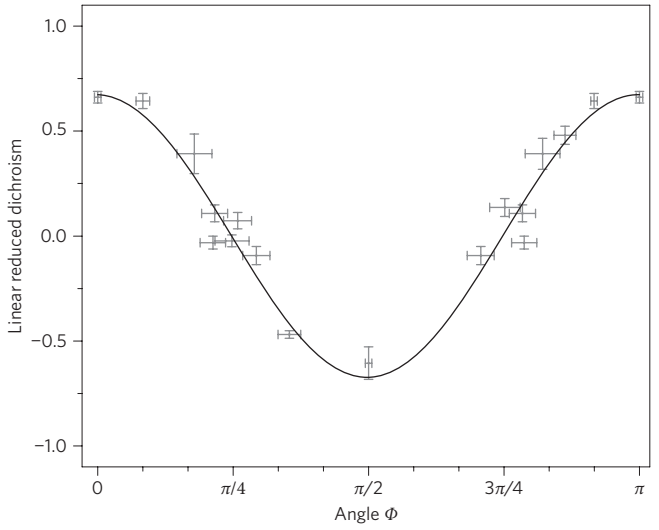

Figure 5 | Fluorescence dichroism of single tubes with different orientation. Plot of the dichroism D of intact single aggregate nanostructures as a function of their orientation characterized by the angle Φ between the aggregate and the horizontal x-axis within the detection plane (for error bars see Supplementary Information). The fit to the data points shows the expected $\cos 2\Phi$ dependence, with an amplitude of 0.67.

for C8S3 tubular aggregates prepared along a similar route[5], which revealed that the molecules were packed in the walls with their transition dipole moments at an angle of ∼45° to the tubes' axis and energy separations between the exciton states on the order of a few hundred cm^{-1}. The total fluorescence at room temperature is biased towards the parallel components, which correspond to the lower energy transitions, but the energy separation of $\sim k_B T$ still allows a small portion of the emission to emanate from the higher energy perpendicular transitions.

The emission selection rules quoted above may break down, even for perfectly uniform structures, because disorder in the molecular transition energies and interactions, imposed by random fluctuations in the environment, breaks the cylindrical symmetry of the exciton system[26]. This leads to localization of the exciton states on finite patches on the tubes' walls. If the NSOM resolution does not allow excitation of individual exciton states, equation (2) still holds, where a is effectively averaged over disorder realizations. An interesting challenge will be to experimentally probe the possible role of disorder and exciton localization by locally measuring the fluorescence emission or excitation spectra or locally probing the exciton dynamics[4,27–29] on individual aggregates.

The immobilization of uniform double-walled tubes from solution also opens the exciting perspective to study exciton transport, a crucial property for applications such as light harvesting, in individual well-defined aggregates. So far such studies have been limited to ensembles of aggregates (often of unknown morphology) with random exciton traps. These studies could not answer questions regarding the nature and range of the exciton motion in individual aggregates. For these double-walled aggregates, the typical strength of the excitonic interactions and the exciton lifetime suggest transport lengths between 30 nm (diffusive Förster regime) and 1 μm (unidirectional coherent motion) (see Supplementary Information). Partial coherence, as reflected by the sharp J-bands, leads to the expectation that this length is of the order of 100 nm. Our work makes it possible to directly verify this in future experiments by optically probing individual uniform immobilized aggregates on the nanoscale.

In summary, individual nanotubular J-aggregates, self-assembled in solution, have been immobilized on solid substrates without destroying their delicate double-walled nanostructure. Polarization-resolved fluorescence NSOM reveals that their supramolecular structure is highly uniform both along an individual tube and between different tubes within an ensemble, even after deposition. This makes them excellent model systems for the investigation of exciton transport in individual quasi-one-dimensional nanostructures as well as for light harvesting and other optoelectronic applications in future solid-state devices.

Methods

Preparation of J-aggregates. The amphiphilic cyanine dye derivative 3,3′-bis(2-sulphopropyl)-5,5′,6,6′-tetrachloro-1,1′-dioctylbenzimidacarbocyanine (C8S3, $M_W = 902.8$ g mol^{-1}, scheme 1a) was obtained as a sodium salt (FEW Chemicals) and used as received. Double-walled nanotubular J-aggregates were prepared according to the 'alcoholic route'[7] as described in detail elsewhere[19].

Deposition and characterization. To immobilize isolated individual nanotubular J-aggregates on a solid substrate, a drop-flow technique was developed as follows. The substrates were cleaned with ammonium hydroxide and hydrogen peroxide and stored in ultrapure water. About 100 μl J-aggregate solution was poured over a tilted (∼80° with respect to the horizontal) cleaned glass or quartz slide of ∼1 cm × 1 cm, and then slowly dried in air for ∼1 h while stored in a black box in order to isolate the J-aggregates on the surface completely from air currents and light.

Fluorescence spectra of both J-aggregates on quartz surfaces and in solution were taken with a fluorescence spectrometer (Shimadzu RF-5001PC) in a 0.1-mm quartz cell (Hellma) with an excitation wavelength of 530 nm.

The morphology of J-aggregates deposited on solid substrates was investigated by scanning force microscopy (SFM) using a MultiMode™ SFM (Veeco Instruments) operated under ambient conditions in tapping mode™. OLYMPUS etched silicon cantilevers were used that had a typical resonance frequency in the range 200–400 kHz and a spring constant of ∼42 N m^{-1}.

Line scans on height images revealed two different apparent heights, (6±1) nm and (18±2) nm (see Supplementary Information). However, they cannot be attributed directly to the thickness of the adsorbed nanostructures, because the material properties of adsorbate and substrate cause different adhesion and also wetting behaviours of, for example, water from the ambient humidity[30], so a better approach to the thicknesses is the evaluation of the difference in thickness of the observed two adsorbed nanostructures. This difference amounts to (12±2) nm, which is in good agreement with the diameter of the individual nanotubes of (13±0.5) nm, determined from cryoTEM images of frozen solutions[7].

The fluorescence spectrum of the adsorbed nanotube ensemble (Fig. 2b) strongly suggests that the supramolecular structure of the nanotubes is unchanged upon deposition on the solid substrates. We therefore exclude a significant deformation of the nanotube's circumference, even though the apparent height of the smallest objects is much lower than the diameter of the nanotube in solution. Instead, we attribute the apparent height to an offset of the absolute height scale by ∼6 nm. This makes the absolute thickness of the larger objects (24±2) nm, corresponding to a double layer of individual tubes. The tube's cross-section is difficult to determine from the SFM images due to the convolution of the tip apex with the sample shape. If one compares the fluorescence intensity of the thicker tubular objects with the thinner ones, a ratio of 4±1 is observed (see Supplementary Information). Given the lack of quenching observed for the merging aggregates in Fig. 3e,f, one can conclude that the thicker nanostructures are bundles of four individual tubes. Such bundles are also observed in the frozen aggregate solution by cryoTEM[7].

Polarization-resolved emission NSOM. NSOM images were collected using an Aurora NSOM from TopoMetrix™ Cooperation (Veeco Instruments) modified for polarized fluorescence imaging[21]. Both topography and near-field fluorescence images were collected simultaneously. The topography images were measured by monitoring the shear-force signal of the tip interacting with the substrate. High-resolution fluorescence images were collected by illuminating the sample with the NSOM probe and collecting the excited fluorescence in the far-field. Laser light (532 nm) was coupled into an aluminium-coated NSOM probe that had been mounted on a tuning fork, supplied by Veeco Instruments. An image was generated by raster scanning the NSOM probe across the sample with a dwell time of 40 ms for each pixel. The J-aggregate emission was collected from below the sample with a microscope objective (NA = 0.7). The fluorescence signal was separated from the excitation light using an optical broadband filter. Finally, the emission was focused by a lens system through a broadband polarizing cube beamsplitter (Newport Cooperation, 05FC16PB.3, T_p/T_s 1,000:1 average) onto the front of two single photon counting avalanche photodiodes (PerkinElmer SPCM-AQ 14) to detect the two orthogonal polarizations. The polarization-resolved beamsplitter (analyser) was aligned such that the polarization directions corresponded to the axes of the scanning stage and thus to the image frame. The optical resolution was quantified from line-scans across individual aggregate features (see Supplementary Information). Based on the full-width at half-maximum (FWHM) of the line scans, it was better than 70 nm, on the order of $\lambda/8$. This may be limited by the pixel size of 66.7 nm (300 × 300 data points for a 20 μm × 20 μm image). The given resolution is more than sufficient to probe single tubular aggregates on the surfaces.

Received 8 May 2009; accepted 15 July 2009;
published online 30 August 2009

References

1. Scholes, G. D. & Rumbles, G. Excitons in nanoscale systems. *Nature Mater.* **5,** 683–696 (2006).
2. Hoeben, F. J. M., Jonkheijm, P., Meijer, E. W. & Schenning, A. P. H. J. About supramolecular assemblies of π-conjugated systems. *Chem. Rev.* **105,** 1491–1546 (2005).
3. Hofmann, C. *et al.* Single-molecule study of the electronic couplings in a circular array of molecules: light-harvesting-2 complex from rhodospirillum molischianum. *Phys. Rev. Lett.* **90,** 013004 (2003).
4. Lang, E., Sorokin, A., Drechsler, M., Malyukin, Y. V. & Köhler, J. Optical spectroscopy on individual amphi-pic j-aggregates. *Nano Lett.* **5,** 2635–2640 (2005).
5. Didraga, C. *et al.* Structure, spectroscopy and microscopic model of tubular carbocyanine dye aggregates. *J. Phys. Chem. B* **108,** 14976–14985 (2004).
6. Röger, C., Miloslavina, Y., Brunner, D., Holzwarth, A. R. & Würthner, F. Self-assembled zinc chlorin rod antennae powered by peripheral light-harvesting chromophores. *J. Am. Chem. Soc.* **130,** 5929–5939 (2008).
7. von Berlepsch, H., Kirstein, S., Hania, R., Pugzlys, A. & Böttcher, C. Modification of the nanoscale structure of the j-aggregate of a sulfonate-substituted amphiphilic carbocyanine dye through incorporation of surface-active additives. *J. Phys. Chem. B* **111,** 1701–1711 (2007).
8. Psencik, J., Ma, Y.-Z., Arellano, J. B., Hala, J. & Gillbro, T. Excitation energy transfer dynamics and excited-state structure in chlorosomes of chlorobium phaeobacteroides. *Biophys. J.* **84,** 1161–1179 (2003).
9. Beljonne, D. *et al.* Excitation migration along oligophenylenevinylene-based chiral stacks: delocalization effects on transport dynamics. *J. Phys. Chem. B* **109,** 10594–10604 (2005).
10. Yamamoto, Y. *et al.* Photoconductive coaxial nanotubes of molecularly connected electron donor and acceptor layers. *Science* **314,** 1761–1764 (2006).
11. Kaiser, T. E., Wang, H., Stepanenko, V. & Würthner, F. Supramolecular construction of fluorescent j-aggregates based on hydrogen-bonded perylene dyes. *Angew Chem. Int. Ed.* **46,** 5541–5544 (2007).
12. Cacialli, F. *et al.* Cyclodextrin-threaded conjugated polyrotaxanes as insulated molecular wires with reduced interstrand interactions. *Nature Mater.* **1,** 160–164 (2002).
13. Samori, P., Francke, V., Müllen, K. & Rabe, J. P. Self-assembly of a conjugated polymer: from molecular rods to a nanoribbon architecture with molecular dimensions. *Chem. Eur. J.* **5,** 2312–2317 (1999).
14. Bredas, J. L., Beljonne, D., Coropceanu, V. & Cornil, J. Charge-transfer and energy-transfer processes in π-conjugated oligomers and polymers: a molecular picture. *Chem. Rev.* **104,** 4971–5003, (2004).
15. Jahnke, E., Severin, N., Kreutzkamp, P., Rabe, J. P. & Frauenrath, H. Molecular level control over hierarchical structure formation and polymerization of oligopeptide–polymer conjugates. *Adv. Mater.* **20,** 409–414, (2008).
16. De Rossi, U., Dähne, S., Meskers, S. C. J. & Dekkers, H. P. J. M. Spontaneous formation of chirality in j-aggregates showing Davydov splitting. *Angew Chem. Int. Ed. Engl.* **35,** 760–763 (1996).
17. Oostergetel, G. T. *et al.* Long-range organization of bacteriochlorophyll in chlorosomes of Chlorobium tepidum investigated by cryo-electron microscopy. *FEBS Lett.* **581,** 5435–5439 (2007).
18. Balaban, T. S., Tamiaki, H. & Holzwarth, A. R. in *Supermolecular Dye Chemistry* (ed. F. Würthner) 1–38 (Topics in Current Chemistry Vol. 258, Springer Verlag, 2005).
19. Lyon, J. L. *et al.* Spectroelectrochemical investigation of double-walled tubular j-aggregates of amphiphilic cyanine dyes. *J. Phys. Chem. C* **112,** 1260–1268 (2008).
20. Higgins, D. A., Kerimo, J., Vanden Bout, D. A. & Barbara, P. F. A molecular yarn: near-field optical studies of self-assembled, flexible, fluorescent fibers. *J. Am. Chem. Soc.* **118,** 4049–4058 (1996).
21. Teetsov, J. A. & Vanden Bout, D. A. Imaging molecular and nanoscale order in conjugated polymer thin films with near-field scanning optical microscopy. *J. Am. Chem. Soc.* **123,** 3605–3606 (2001).
22. Taminiau, T. H., Stefani, F. D., Segerink, F. B. & Van Hulst, N. F. Optical antennas direct single-molecule emission. *Nature Photon.* **2,** 234–237 (2008).
23. Hamanaka, Y., Kawasaki, O., Yamauchi, T. & Nakamura, A. Morphology of self-assembled merocyanine j-aggregates in films studied by scanning near-field optical microscope. *Chem. Phys. Lett.* **378,** 47–54 (2003).
24. Vacha, M. *et al.* Optical properties of individual nanostructures of molecular j-aggregates. *J. Lumin.* **98,** 35–40 (2002).
25. Malyukin, Y. V., Sorokin, A. V., Yefimova, S. L. & Lebedenko, A. Photo-induced reorganization of molecular packing of amphi-pic j-aggregates (single j-aggregate spectroscopy). *J. Lumin.* **112,** 429–433 (2005).
26. Didraga, C. & Knoester, J. Optical spectra and localization of excitons in inhomogeneous helical cylindrical aggregates. *J. Chem. Phys.* **121,** 10687–10698 (2004).
27. Hofmann, C., Aartsma, T. J., Michel, H. & Köhler, J. Direct observation of tiers in the energy landscape of a chromoprotein: a single-molecule study. *Proc. Natl Acad. Sci. USA* **100,** 15534–15538 (2003).
28. Cotlet, M. *et al.* Identification of different emitting species in the red fluorescent protein DsRed by means of ensemble and single-molecule spectroscopy. *Proc. Natl Acad. Sci. USA* **98,** 14398–14403 (2001).
29. Hernando, J. *et al.* Effect of disorder on ultrafast exciton dynamics probed by single molecule spectroscopy. *Phys. Rev. Lett.* **97,** 216403 (2006).
30. Zhuang, W. *et al.* SFM characterization of poly(isocyanodipeptide) single polymer chains in controlled environments: effect of tip adhesion and chain swelling. *Macromolecules* **38,** 473–480 (2005).

Acknowledgements

Financial support for this work was provided by the R.A. Welch Foundation (grant no. F-1377) and Deutsche Forschungsgemeinschaft (Sfb 448 Mesoscopically Organized Composites).

Author contributions

J.P.R. and D.A.V.B. directed the project. D.M.E. performed sample preparation and ensemble experiments, supervised by J.P.R., performed the near-field experiments and their data analysis under the guidance of D.A.V.B. and initiated the collaboration. J.K. contributed to data analysis and played an important role in putting the measurements in perspective. S.K. provided helpful discussions and beneficial interpretation of the data analysis. D.M.E., J.K. and D.A.V.B. co-wrote the paper, with input from the other authors.

Additional information

Supplementary information accompanies this paper at www.nature.com/naturenanotechnology. Reprints and permission information is available online at http://npg.nature.com/reprintsandpermissions/. Correspondence and requests for materials should be addressed to J.P.R. and D.A.V.B.